# Model Predictive Control in Power Electronics: Strategies to Reduce the Computational Complexity

Petros Karamanakos[*], Tobias Geyer[†], Nikolaos Oikonomou[†], Frederick Kieferndorf[†], and Stefanos Manias[‡]

[*]Institute for Electrical Drive Systems and Power Electronics, Technische Universität München, Munich, Germany
Email: [*]p.karamanakos@ieee.org
[†]ABB Corporate Research, Baden-Dättwil, Switzerland
Email: [†]t.geyer@ieee.org, nikolaos.oikonomou@ch.abb.com, frederick.kieferndorf@ch.abb.com
[‡]Department of Electrical and Computer Engineering, National Technical University of Athens, Athens, Greece
Email: [‡]manias@central.ntua.gr

*Abstract*—**Model predictive control (MPC) is a control strategy that has been gaining more and more attention in the field of power electronics. However, in many cases the computational requirements of the derived MPC-based algorithms are difficult to meet, even with modern microprocessors that are immensely powerful and capable of executing complex instructions at a faster rate than ever before. To overcome this difficulty, three strategies that can significantly reduce the complexity of computationally demanding MPC schemes are presented in this paper. Three case studies are examined in order to verify the effectiveness of the proposed strategies. These include a move blocking strategy for a dc-dc boost converter and both an extrapolation strategy and an event-based horizon strategy for a dc-ac medium-voltage (MV) drive.**

## I. Introduction

Power electronics is a mature technology that has been in use for more than four decades. From air-conditioners to rail transport and from mobile phones to motor drives, power electronics circuits have proved indispensable in many areas because they convert electrical power from one form to another, such as ac-dc, dc-dc, dc-ac, or even ac-ac with a variable output magnitude and frequency [1].

Over the years many control strategies for power electronics have been proposed that have been shown to be reasonably effective. Mainly, these are strategies based on linear controllers combined with nonlinear techniques, such as pulse width modulation (PWM). However, controllers of this type are usually tuned to achieve optimal performance only over a narrow operating range; outside this range the performance is significantly deteriorated. Therefore, the problems associated with many applications and their closed-loop controlled performance still poses theoretical and practical challenges. Furthermore, the advent of new applications leads to the need for new control approaches that will meet the increasingly demanding performance requirements.

A control algorithm that has been recently gaining more popularity in the field of power electronics is model predictive control (MPC) [2], [3]. This control method, which has been successfully used in the process industry since the 1970s, has attracted the interest and attention of research and academic communities due to its numerous advantageous features, such as design simplicity, explicit inclusion of design criteria and restrictions, fast dynamics and inherent robustness. In addition, the emergence of fast microprocessors has increasingly enabled successful implementation [4]–[8].

In MPC, an optimization problem is formulated based on an objective function that captures the control objectives over a finite prediction horizon. The control action is determined by minimizing in real-time and at every time-step the chosen objective function, subject to the discrete-time model of the system and constraints. The sequence of control inputs with the minimum associated cost is the *optimal* solution. Out of this sequence only the first element is applied to the converter. In the next sampling instant, all the variables are shifted by one sampling interval and the optimization problem is repeated based on new measurements or estimates. This procedure is known as the *receding horizon policy* [9]. In this way feedback is provided, allowing one to cope with model uncertainties and disturbances.

However, MPC-based algorithms are very challenging to implement because of the high level of computation required. In general, the computational complexity—depending on the type of the optimization problem—grows exponentially with the length of the prediction horizon and the number of the manipulated variables [10], [11]. One solution to reduce the number of computations is to keep the horizon as short as possible, i.e. to employ a one-step horizon. Unfortunately, in many control problems a long prediction horizon is needed to sufficiently predict the behavior of the state and output variables for adequate performance, as well as to avoid stability problems [12]. Thus, for such problems one must find methods of predicting over long horizons to improve plant performance while reducing the complexity of the calculations so the implementation of the algorithm is possible in real systems.

In this survey paper existing efficient computational strategies for addressing large-scale MPC problems in power electronics are highlighted. More specifically, three techniques that reduce the complexity of MPC are shown: move blocking, extrapolation, and event-based horizons. In addition, illustrative examples are presented in order to show how the aforementioned strategies are applied, as well as their effectiveness. The first strategy is demonstrated with a dc-dc boost converter, while the other two are applied to a dc-ac medium-voltage (MV) drive.
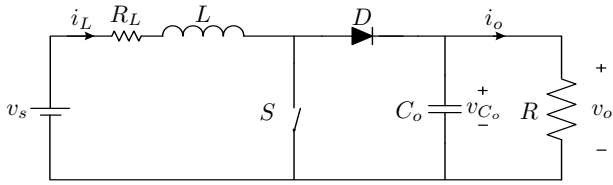
Fig. 1: Topology of the dc-dc boost converter, where $v_s$ is the input voltage, $v_o$ is the output voltage over the load resistor $R$, which is considered equal to the voltage $v_{C_o}$ across the capacitor $C_o$, $i_L$ is the current through the inductor $L$ (the inductor has an internal resistance $R_L$) and $S$ and $D$ are two power switches: $S$ is controllable and $D$ (diode) is uncontrollable.

## II. MOVE BLOCKING STRATEGY

A *move blocking* strategy [13] is used to emulate a long prediction horizon, while the computational complexity is kept modest. According to this method, a long horizon with only a few prediction steps $N \in \mathbb{N}^+$ can be achieved. The prediction horizon is split into two parts; $N_1$ are the prediction steps in the first part of the horizon, and $N_2$ the steps in the last part. Thus, the total number of time-steps in the horizon is $N = N_1 + N_2$. For the $N_1$ steps the model is sampled with a sampling interval $T_s$, while for the $N_2$ steps, i.e. the steps far in the future, the model is sampled more coarsely with a multiple of $T_s$, i.e. $n_s T_s$, with $n_s \in \mathbb{N}^+$ [14]. As a result, by using different sampling intervals within the prediction horizon, a long horizon is achieved.

As a case study, consider the dc-dc boost converter shown in Fig. 1. This converter is capable of producing a controlled dc output voltage greater in magnitude than the typically uncontrolled dc input voltage. The control objective is for the output voltage to accurately track its reference value despite changes in the input voltage or the load. However, directly controlling the output voltage without an intermediate current control loop [15] is not a trivial task. This is due to the fact that the output voltage exhibits a nonminimum phase behavior with respect to the control input. For example, when the output voltage reference is increased, the duty cycle should also increase, but initially the output voltage drops before it begins to rise again. This means that the sign of the gain (from the duty cycle to the output voltage) is not always positive.

Therefore, a sufficiently long prediction interval $NT_s$ is required, in order for the controller to "see" beyond the initial voltage drop and thus to ensure closed-loop stability. Based on the discussion above, a long prediction interval can be achieved with a significant reduction of required computations by employing a move blocking strategy, as shown in [16]. An example of dividing the horizon into two parts relative to the output voltage, input current and control input is shown in Fig. 2.

In Fig. 3 an example of the effectiveness of the move blocking strategy is illustrated. At step $k$ the output voltage reference is increased. However, due to the nonminimum phase nature of the system, the output voltage initially decreases. Therefore, a multiple-step prediction horizon is needed to ensure that MPC is able to predict the final voltage increase and thus choose the proper control actions that will achieve this. In the example of Fig. 3 a twenty time-step horizon is required ($N = 20$) so that the controller will "see" the positive
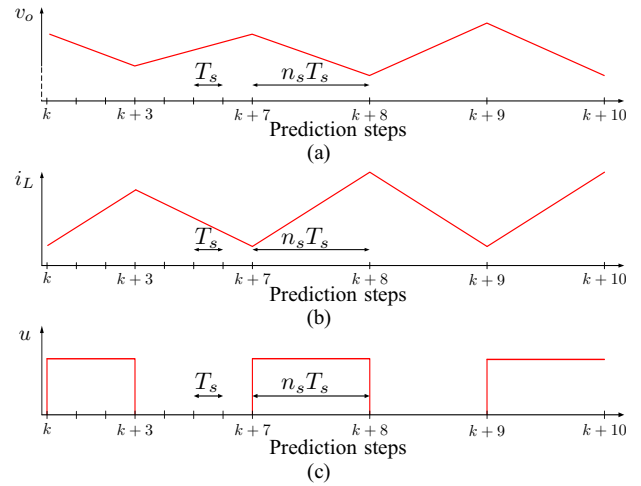


Fig. 2: Prediction horizon with move blocking: a) output voltage, b) inductor current and c) control input. The prediction horizon has $N = 10$ time-steps, but the prediction interval is of length $19T_s$, since $n_s = 4$ is used for the last $N_2 = 3$ steps.
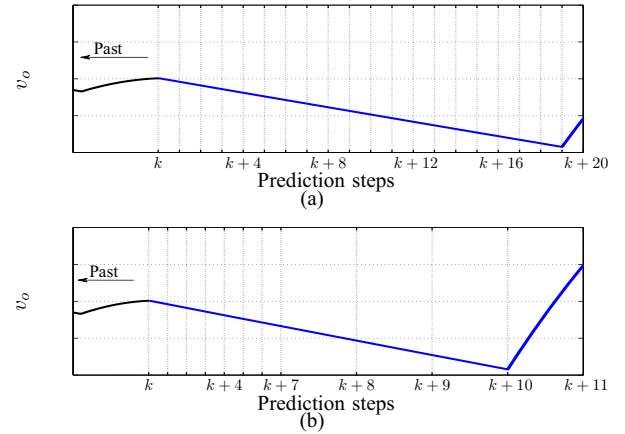


Fig. 3: Effect of the move blocking scheme. In (a), without move blocking, a prediction horizon of $N = 20$ steps of equal time-intervals is needed. In (b), with the move blocking strategy employed, an $N = 11$ prediction horizon is sufficient to achieve the same closed-loop result ($N_1 = 7$, $N_2 = 4$ and $n_s = 4$, total length $23T_s$).

slope of the voltage, meaning that the number of control input sequences to be examined is $2^{20} = 1048576$[1] and the state evolution has to be predicted for 20 steps into the future.

If the move blocking strategy is adopted, then a prediction interval of eleven time-steps $NT_s = 11$, with $N_1 = 7$, $N_2 = 4$ and $n_s = 4$ will suffice; the resulting prediction interval will be 23 steps long. This means that the total number of sequences will be $2^{11} = 2048$ and the evolution of the state will be calculated only for 11 steps. As a result, the computations required are decreased by three orders of magnitude, or $99.9\%$.

To evaluate the performance of the closed-loop system, in Fig. 4 a step-down change in the output reference voltage is investigated experimentally. A six-step prediction horizon is implemented, i.e. $N = 6$ and the sampling interval is $T_s = 10\,\mu$s. The prediction horizon is split into $N_1 = 4$ and $N_2 = 2$ with $n_s = 2$. The output reference voltage changes

[1]For this example, enumeration strategy is used to solve the optimization problem. According to this strategy, the controller has to examine $2^N$ sequences at every iteration [16].
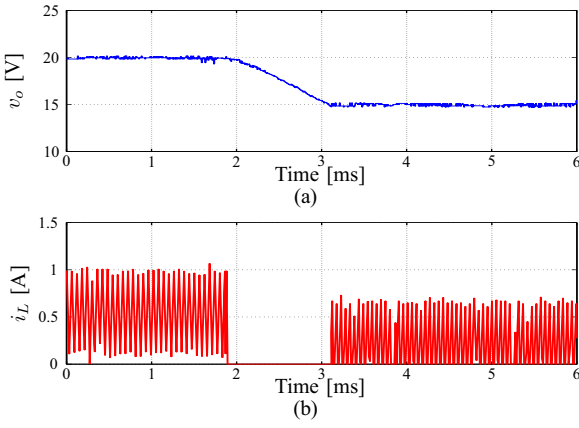
Fig. 4: Closed-loop performance during a step-down change in the output voltage reference: a) output voltage and b) inductor current (experimental results—Parameters: $v_s = 10\,\text{V}$, $L = 450\,\mu\text{H}$, $R_L = 0.3\,\Omega$, $C_o = 220\,\mu\text{F}$, and $R = 73\,\Omega$).

from $v_{o,\text{ref}} = 20\,\text{V}$ to $v_{o,\text{ref}} = 15\,\text{V}$ at $t \approx 1.9\,\text{ms}$. As can be seen the inductor current is instantly reduced to zero so as to allow the capacitor to discharge through the resistor and the converter reaches the new steady-state operating point in about $t \approx 1.2\,\text{ms}$.

## III. EXTRAPOLATION STRATEGY

Another option to ensure a manageable level of complexity is to use *extrapolation* [17]–[22]. The motivation of using this strategy is similar to that presented in Section II, i.e. the horizon must be relatively short, but, at the same time, long enough to accurately capture the dynamics of the variables of concern. To implement the extrapolation strategy—in contrast to the move blocking scheme—soft constraints[2], implemented as hysteresis bounds, on the variables of interest should be present.

To realize the extrapolation strategy, two types of horizons are defined: the switching horizon $N_s \in \mathbb{N}^+$ and the prediction horizon $N_p \in \mathbb{N}^+$, with $N_p \geq N_s$, since the prediction horizon includes the switching horizon. The switching horizon $N_s$, the length of which is set by the designer, is defined as the time interval wherein the state of the converter switches can change. The evolution of the controlled variables is calculated over this short horizon for all control input sequences, creating trajectories. The most "promising" of these trajectories [17] are extrapolated. The length of the prediction horizon $N_p$ is determined by the result of this extrapolation; its upper limit is the time-step where the first controlled variable hits a bound. From step $k + N_s + 1$ to $k + N_p - 1$ it is assumed that the state of the switches stays the same.

As a case study, consider the five-level active neutral point clamped (ANPC-5L) inverter shown in Fig. 5 with an induction machine (IM) as the load. The ANPC-5L inverter is capable of producing the following phase to neutral normalized voltage levels $\{-2, -1, 0, +1, +2\}$, resulting in $5^3 = 125$ possible three-phase voltage vectors. These vectors produce 61 unique line-to-line output voltage vectors; each set of three-phase voltage vectors which produce the same output voltage
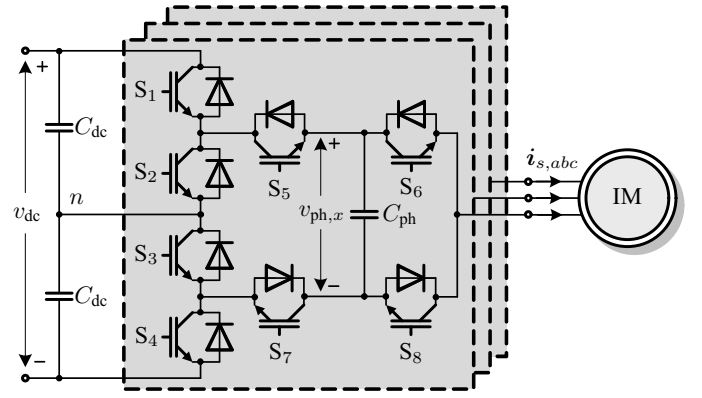
Fig. 5: Circuit diagram of the five-level active neutral point clamped (ANPC-5L) voltage source inverter driving an induction machine (IM).
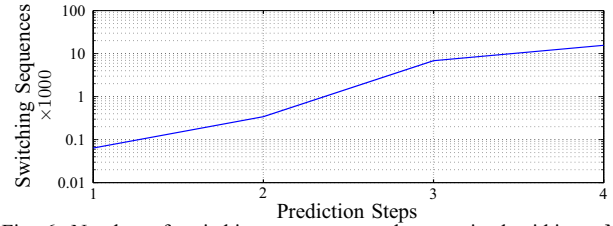


Fig. 6: Number of switching sequences to be examined within a $N_p$-step prediction horizon, with $N_p = \{1, 2, 3, 4\}$, for the case of a ANPC-5L inverter, when the switching constraints are taken into account.

is termed a three-phase redundancy [23]. Moreover, single-phase redundancies exist: the phase leg of the ANPC-5L inverter has eight allowed switching states that can produce the five unique phase to neutral voltage levels [23]. Hence, $8^3 = 512$ three-phase vectors can be produced. The control objective is to effectively exploit the topology redundancies, i.e. to use the 512 three-phase voltage vectors, so as to keep the neutral point $v_n$ and phase capacitor voltages $v_{\text{ph},x}$, with $x = \{a, b, c\}$ (see Fig. 5), inside the given bounds, while operating the converter at the lowest possible switching frequency.

If an exhaustive search of all possible switching transitions from one voltage vector to another is considered, then $512^{N_p}$ sequences, where $N_p = N_s$ is the prediction horizon, must be examined. However, constraints that stem from the topology of the inverter, such as minimum pulse time duration, dc-link clamp restrictions and allowed state transitions of the inverter phase leg, significantly reduce the allowable (or *feasible*) sequences. According to the sequences generation algorithm presented in [22], the number of sequences that must be evaluated in a $N_p$-step prediction horizon, with $N_p = \{1, 2, 3, 4\}$, is shown in Fig. 6. As can be seen, when a three-step horizon is employed ($N_p = 3$), there are 6859 sequences to be examined. Thus, the implementation of an MPC algorithm, even with a relatively short horizon, in a real-time system is an impossible task.

However, using a two-step switching horizon, i.e. $N_s = 2$ with the extrapolation strategy, a twofold task is achieved: only 343 sequences are generated and the prediction length is improved, since a long prediction horizon is approximated. In Fig. 7 trajectories that can stand either for the neutral point $v_{n,\text{err}} = v_{n,\text{ref}} - v_n$, or the phase capacitor $v_{\text{ph},x,\text{err}} = v_{\text{ph},x,\text{ref}} - v_{\text{ph},x}$ voltage error are illustrated. The
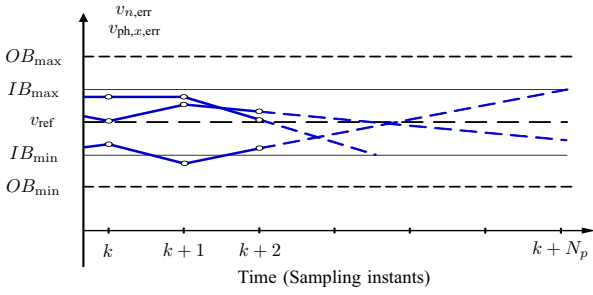
Fig. 7: Examples of internal voltage switching trajectories that illustrate the effect of extrapolation. The switching horizon is $N_s = 2$. The internal voltages are extended by linearly extrapolating the predicted voltage values from steps $k+1$ and $k+2$. For the case of the ANPC-5L inverter two different bounds are required and illustrated here: the inner bounds ($IB$) are defined by the desired maximum absolute deviation from the respective reference voltage values and the outer bounds ($OB$) are set by the allowed physical limits of the semiconductor devices.
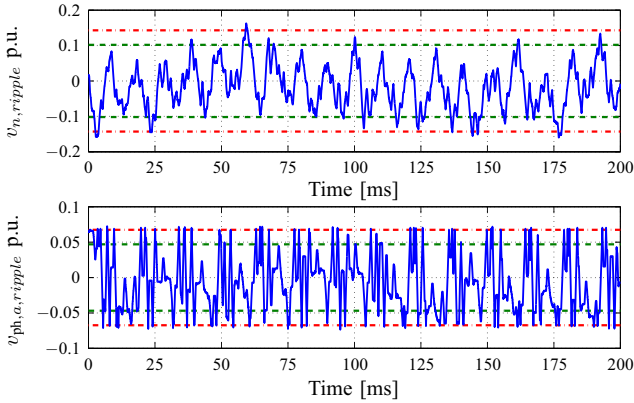


Fig. 8: Simulation results for the per unit ripple of internal voltages with the inner (green) and outer (red) bounds. Operating point: 65% speed (32 Hz), 42% load.

switching horizon is selected to be $N_s = 2$, while the prediction horizon depends on the final slope of each trajectory. The optimal trajectory is then defined to correspond to the sequence of control moves that minimizes a specified objective function. In [22] different approaches to the control problem presented here, as well as various formulations of objective functions based on certain selection criteria are introduced.

The performance of the MPC algorithm presented in [22] is tested using a 1 MVA ACS 2000 MV drive from ABB coupled to a 6-kV, 137-A IM driving a quadratic torque load. In order to successfully implement the algorithm, a two-step switching horizon ($N_s = 2$, $T_s = 25\,\mu$s) with an extrapolation strategy is employed. In Fig. 8 the waveforms of the voltages of the neutral point and the phase capacitor of phase $a$ are depicted. Furthermore, the switching frequency is kept low over the whole operating regime, as shown in Fig. 9.

## IV. EVENT-BASED HORIZON

Recently, a new control approach has been applied to a MV ac drive system [24]. The concept of optimal pulse patterns (OPPs) [25] is adopted in combination with MPC. OPPs are calculated such that the total harmonic distortion (THD) of the machine currents is minimized over the linear and nonlinear range of the modulation index. The offline computed OPPs
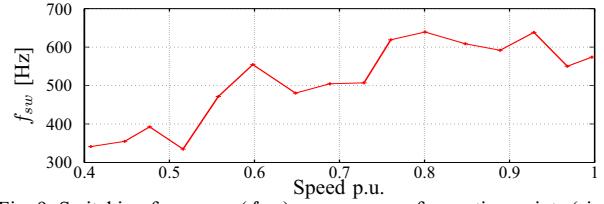


Fig. 9: Switching frequency ($f_{sw}$) over a range of operating points (simulation results).

are used to calculate an optimal stator flux trajectory that the controller tracks in real-time [26]. Thus, the introduced MPC-based algorithm aims to compensate as quickly as possible the flux error in real-time by modifying the offline-calculated switching instants, which are stored in a lookup table, of the OPPs.

However, a relatively long prediction horizon is required for the flux error correction procedure. In order to overcome this obstacle a deadbeat version of the strategy has been proposed [24], where an *event-based* prediction horizon is employed. But, in order to achieve high dynamic performance in closed loop, the deadbeat implementation must be further refined, without exceeding computational limitations based on the length of the prediction horizon. Thereby, in [27] the event-based prediction horizon is reformulated in order to limit the calculations needed without deteriorating the dynamic behavior of the controller.

To make clear how the event-based horizon is implemented, consider the ANCP-5L inverter driving an IM, as shown in Fig. 5. The correction of the flux error $\psi_{s,\mathrm{err}} = \psi_{s,\mathrm{ref}} - \psi_s$, where $\psi_{s,\mathrm{ref}}$ is the reference vector, and $\psi_s$ the estimated vector, is achieved by modifying in real-time the pre-calculated (nominal) switching instants, $t_x^*$, $x \in \{a, b, c\}$, of the OPPs by a time interval $\Delta t_x$, resulting in a modified switching instant $t_x = t_x^* + \Delta t_x$. The volt-second area that the pulse sequence of each phase contributes to the flux is either increased or decreased depending on the direction of the modification and the switching transitions effected [24] (Fig. 10).

The event-based horizon depends on the two future nominal switching instants, $t_{act_1}$ and $t_{act_2}$, which are closest to $t_0 = kT_s$ and the modified switching instants of the involved phases. If the two switching instants that follow $t_0$ occur in different phases, the flux error vector is projected onto these two phases. In this case, two phases in pairs, i.e. $\{a, b\}$, $\{b, c\}$ or $\{c, a\}$, are considered as the active phases in the flux error correction procedure, i.e. two degrees of freedom. On the other hand, if both switching instants $t_{act_1}$ and $t_{act_2}$ that follow $t_0$ occur in the same phase, then this phase is considered as the only active phase, i.e. $a, b$ or $c$. For example, in Fig. 10(a), the two active switching instants $t_{act_1} = t_{b_1}^*$ and $t_{act_2} = t_{a_1}^*$ are in phases $b$ and $a$, respectively. While in Fig. 10(b), only one phase is involved in the flux error correction procedure, since both active switching instants $t_{act_1} = t_{b_1}^*$ and $t_{act_2} = t_{b_2}^*$ are in phase $b$.

The length of the horizon is equal to the maximum difference between the initial sampling instant $t_0$ and the nominal or modified switching instants (Fig. 10), i.e.

$$T_p = \max\{t_x^* - t_0, t_x - t_0\}. \tag{1}$$

(a) The switching instants are the nominal values $t_{act_1} = t^*_{b_1}$ and $t_{act_2} = t^*_{a_1}$; they are shifted to $t_{b_1}$ and $t_{a_1}$, respectively within the horizon $T_p$, shown by the black arrow. At $t = t_{a_1}$, the horizon is reevaluated.

(b) The switching instants are the nominal values $t_{act_1} = t^*_{b_1}$ and $t_{act_2} = t^*_{b_2}$; instant $t^*_{b_1}$ is shifted to $t_{b_1}$ within the horizon $T_p$, shown by the black arrow. At $t = t_{b_1}$, the horizon is reevaluated.
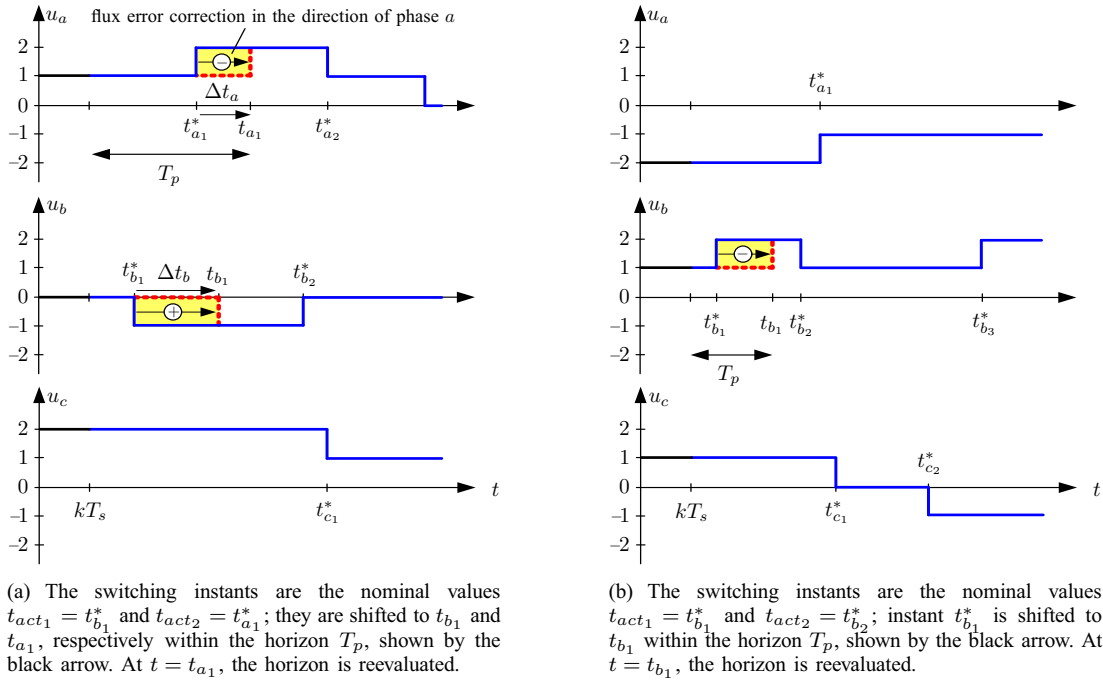
Fig. 10: The MPC controller is activated at time instant $kT_s$ and it modifies pre-calculated switching instants of a three-phase, five-level pulse pattern.
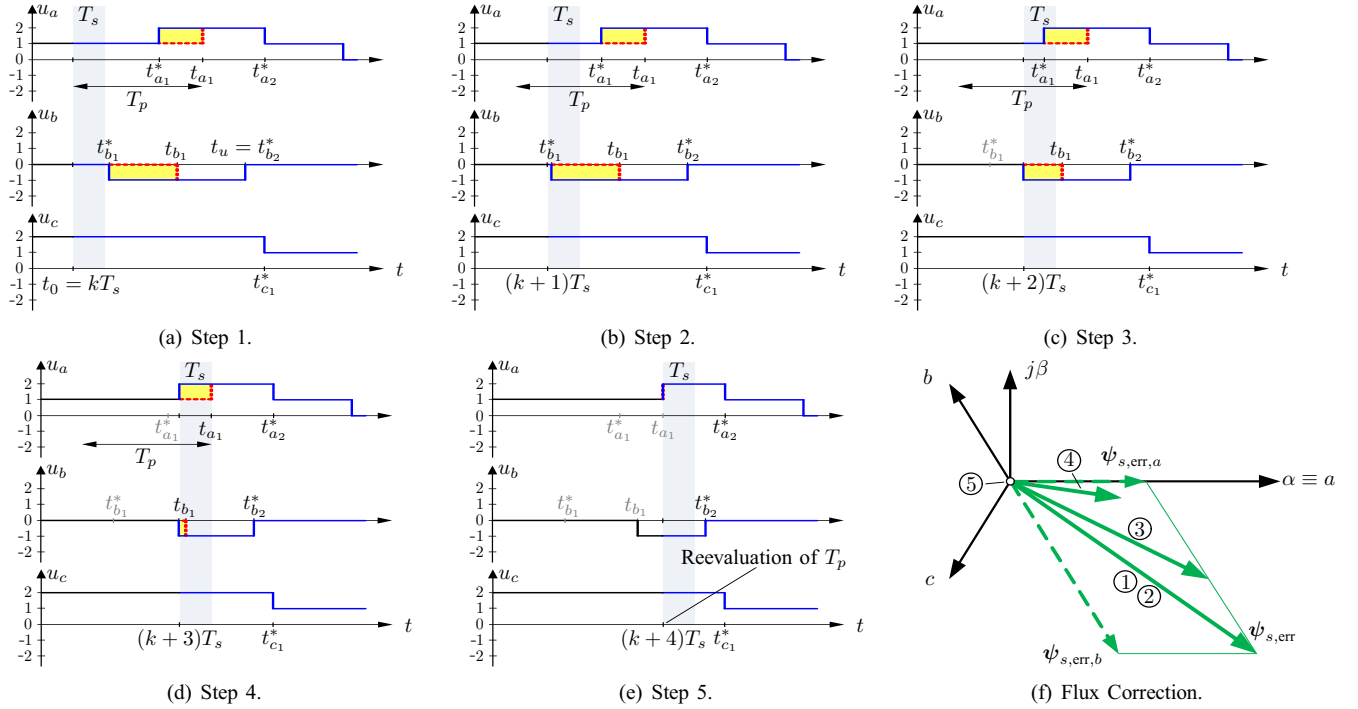


(a) Step 1.

(b) Step 2.

(c) Step 3.

(d) Step 4.

(e) Step 5.

(f) Flux Correction.

Fig. 11: Example of flux error $\boldsymbol{\psi}_{s,\mathrm{err}}$ correction within four sampling intervals $4T_s$. The circled numbers in (f) correspond to the flux error compensation steps shown in (a)–(e).

In Fig. 11 an illustrative example of the flux error correction is shown. The goal is to compensate the flux error $\boldsymbol{\psi}_{s,\mathrm{err}}$ shown as bold solid lines in Fig. 11(f). In Fig. 11(a), the length of the prediction horizon $T_p$ is determined along with the required time modifications $\Delta t_a = -(t^*_{a_1} - t_{a_1})$ and $\Delta t_b = -(t^*_{b_1} - t_{b_1})$ within the first sampling interval $T_s$. The flux correction starts taking effect after the sampling instant $(k+1)T_s$ (Fig. 11(b)) and the error is fully compensated between $(k+3)T_s$ (Fig. 11(d)) and $(k+4)T_s$ (Fig. 11(e)).

As can be seen, in this example the flux error is eliminated in four sampling intervals (Fig. 11(a) to Fig. 11(d)). The new prediction horizon $T_p$ is then determined in Fig. 11(e).

Employing an event-based horizon the modified algorithm presented in [24] was implemented on a 1 MVA ACS 2000 MV drive from ABB coupled to a 6-kV, 137-A IM with a constant mechanical load. The algorithm is executed every $T_s = 25\,\mu\mathrm{s}$. Stator current waveforms recorded in the experimental setup with the drive system are shown in Fig. 12 while the machine
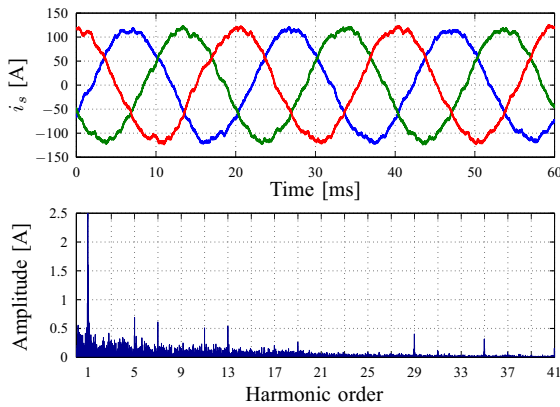
Fig. 12: Experimental results in steady-state operation ($f_1 = 50\,\text{Hz}$ and 62% machine current). Optimal pulse patterns of $d = 10$ switching instants per quarter-wave are employed. Three-phase stator currents and harmonic spectrum are shown; the rms value of the phase current is $85\,\text{A}$. The total demand distortion (TDD) is 3.77% referred to the rated current of the controlled machine ($137\,\text{A}$).

was operated at $50\,\text{Hz}$ frequency and at partial load. The fundamental component of the current was $85\,\text{A}$ rms and the spectrum is zoomed in to focus on the very low amplitudes of the current harmonics. The total demand distortion (TDD) of the stator currents is just 3.77% referred to the rated current of the controlled machine ($137\,\text{A}$).

## V. Conclusions

In this survey paper a number of strategies that can effectively reduce the computational complexity of model predictive control (MPC) algorithms that employ the receding horizon policy have been outlined. Three methods have been considered, namely the move blocking strategy, the extrapolation strategy and the event-based horizon strategy. Furthermore, three examples have been included to highlight the performance of the proposed strategies: dc-dc converters with the move blocking strategy, and ac medium voltage (MV) drives with the extrapolation strategy, and the event-based horizon. These approaches deliver MPC schemes for demanding applications with modest computational costs thus making their implementation possible. An additional major advantage of the presented techniques is that they can easily be modified to meet different control tasks. Thereby, different complex control problems can be successfully tackled by adopting the most suitable strategy.

## References

[1] N. Mohan, T. M. Undeland, and W. P. Robbins, *Power Electronics: Converters, Applications and Design*, 3rd ed.   Hoboken, NJ: Wiley, 2003.
[2] J. M. Maciejowski, *Predictive Control with Constraints*.   Englewood Cliffs, NJ: Prentice-Hall, 2002.
[3] J. B. Rawlings and D. Q. Mayne, *Model Predictive Control: Theory and Design*.   Madison, WI: Nob Hill, 2009.
[4] T. Geyer, "Low complexity model predictive control in power electronics and power systems," Ph.D. dissertation, Autom. Control Lab. ETH Zurich, Zurich, Switzerland, 2005.
[5] P. Cortés, M. P. Kazmierkowski, R. M. Kennel, D. E. Quevedo, and J. Rodríguez, "Predictive control in power electronics and drives," *IEEE Trans. Ind. Electron.*, vol. 55, no. 12, pp. 4312–4324, Dec. 2008.
[6] S. Kouro, P. Cortés, R. Vargas, U. Ammann, and J. Rodríguez, "Model predictive control—A simple and powerful method to control power converters," *IEEE Trans. Ind. Electron.*, vol. 56, no. 6, pp. 1826–1838, Jun. 2009.
[7] A. Linder, R. Kanchan, R. Kennel, and P. Stolze, *Model-based Predictive Control of Electric Drives*.   Göttingen, Germany: Cuvillier Verlag, 2010.
[8] P. Karamanakos, "Model predictive control strategies for power electronics converters and ac drives," Ph.D. dissertation, Elect. Mach. and Power Electron. Lab. NTU Athens, Athens, Greece, 2013.
[9] D. Q. Mayne, J. B. Rawlings, C. V. Rao, and P. O. M. Scokaert, "Constrained model predictive control: Stability and optimality," *Automatica*, vol. 36, no. 6, pp. 789–814, Jun. 2000.
[10] F. Borrelli, "Discrete time constrained optimal control," Ph.D. dissertation, Autom. Control Lab. ETH Zurich, Zurich, Switzerland, 2002.
[11] T. Geyer, "A comparison of control and modulation schemes for medium-voltage drives: Emerging predictive control concepts versus PWM-based schemes," *IEEE Trans. Ind. Appl.*, vol. 47, no. 3, pp. 1380–1389, May/Jun. 2011.
[12] M. Morari and J. H. Lee, "Model predictive control: Past, present and future," *Comput. and Chemical Eng.*, vol. 23, no. 4, pp. 667–682, May 1999.
[13] R. Cagienard, P. Grieder, E. C. Kerrigan, and M. Morari, "Move blocking strategies in receding horizon control," *J. of Process Control*, vol. 17, no. 6, pp. 563–570, Jul. 2007.
[14] T. Geyer, G. Papafotiou, and M. Morari, "Model predictive control in power electronics: A hybrid systems approach," in *Proc. IEEE Conf. Decis. Control*, Seville, Spain, Dec. 2005, pp. 5606–5611.
[15] P. Karamanakos, T. Geyer, and S. Manias, "Direct model predictive current control of dc-dc boost converters," in *Proc. Int. Power Electron. and Motion Control Conf. and Expo.*, Novi Sad, Serbia, Sep. 2012, pp. DS2c.11–1–DS2c.11–8.
[16] ——, "Direct voltage control of dc-dc boost converters using model predictive control based on enumeration," in *Proc. Int. Power Electron. and Motion Control Conf. and Expo.*, Novi Sad, Serbia, Sep. 2012, pp. DS2c.10–1–DS2c.10–8.
[17] T. Geyer, G. Papafotiou, and M. Morari, "Model predictive direct torque control—Part I: Concept, algorithm and analysis," *IEEE Trans. Ind. Electron.*, vol. 56, no. 6, pp. 1894–1905, Jun. 2009.
[18] G. Papafotiou, J. Kley, K. G. Papadopoulos, P. Bohren, and M. Morari, "Model predictive direct torque control—Part II: Implementation and experimental evaluation," *IEEE Trans. Ind. Electron.*, vol. 56, no. 6, pp. 1906–1915, Jun. 2009.
[19] T. Geyer, "Generalized model predictive direct torque control: Long prediction horizons and minimization of switching losses," in *Proc. IEEE Conf. Decis. Control*, Shanghai, China, Dec. 2009, pp. 6799–6804.
[20] ——, "Model predictive direct current control: Formulation of the stator current bounds and the concept of the switching horizon," *IEEE Ind. Appl. Mag.*, vol. 18, no. 2, pp. 47–59, Mar./Apr. 2012.
[21] T. Geyer and S. Mastellone, "Model predictive direct torque control of a five-level ANPC converter drive system," *IEEE Trans. Ind. Appl.*, vol. 48, no. 5, pp. 1565–1575, Sep./Oct. 2012.
[22] F. Kieferndorf, P. Karamanakos, P. Bader, N. Oikonomou, and T. Geyer, "Model predictive control of the internal voltages of a five-level active neutral point clamped converter," in *Proc. IEEE Energy Convers. Congr. Expo.*, Raleigh, NC, Sep. 2012, pp. 1676–1683.
[23] F. Kieferndorf, M. Basler, L. A. Serpa, J.-H. Fabian, A. Coccia, and G. A. Scheuer, "A new medium voltage drive system based on ANPC-5L technology," in *Proc. IEEE Int. Conf. Ind. Technol.*, Viña del Mar, Chile, Mar. 2010, pp. 643–649.
[24] T. Geyer, N. Oikonomou, G. Papafotiou, and F. D. Kieferndorf, "Model predictive pulse pattern control," *IEEE Trans. Ind. Appl.*, vol. 48, no. 2, pp. 663–676, Mar./Apr. 2012.
[25] H. S. Patel and R. G. Hoft, "Generalized techniques of harmonic elimination and voltage control in thyristor inverters: Part I—Harmonic elimination," *IEEE Trans. Ind. Appl.*, vol. IA-9, no. 3, pp. 310–317, May 1973.
[26] J. Holtz and N. Oikonomou, "Synchronous optimal pulsewidth modulation and stator flux trajectory control for medium-voltage drives," *IEEE Trans. Ind. Appl.*, vol. 43, no. 2, pp. 600–608, Mar./Apr. 2007.
[27] N. Oikonomou, C. Gutscher, P. Karamanakos, F. Kieferndorf, and T. Geyer, "Model predictive pulse pattern control for the five-level active neutral point clamped inverter," in *Proc. IEEE Energy Convers. Congr. Expo.*, Raleigh, NC, Sep. 2012, pp. 129–136.